



ELSEVIER

Contents lists available at ScienceDirect

C. R. Acad. Sci. Paris, Ser. I

www.sciencedirect.com



Partial differential equations/Numerical analysis

Asymptotic Preserving numerical schemes for multiscale parabolic problems



Schémas numériques Asymptotic Preserving pour les problèmes paraboliques multi-échelles

Nicolas Crouseilles^{a,c}, Mohammed Lemou^{b,c}, Gilles Vilmart^d^a INRIA, France^b CNRS, France^c IRMAR, Université de Rennes-1, campus de Beaulieu, F-35042 Rennes Cedex, France^d Université de Genève, Section de mathématiques, 2–4, rue du Lièvre, CP 64, CH-1211 Genève 4, Switzerland

ARTICLE INFO

Article history:

Received 27 July 2015

Accepted after revision 19 November 2015

Available online 4 February 2016

Presented by Olivier Pironneau

ABSTRACT

We consider a class of multiscale parabolic problems with diffusion coefficients oscillating in space at a possibly small scale ε . Numerical homogenization methods are popular for such problems, because they capture efficiently the asymptotic behavior as $\varepsilon \rightarrow 0$, without using a dramatically fine spatial discretization at the scale of the fast oscillations. However, it is known that such homogenization schemes are in general not accurate for both the highly oscillatory regime $\varepsilon \rightarrow 0$ and the non-oscillatory regime $\varepsilon \sim 1$. In this paper, we introduce an Asymptotic Preserving method based on an exact micro–macro decomposition of the solution, which remains consistent for both regimes.

© 2015 Académie des sciences. Published by Elsevier Masson SAS. All rights reserved.

R É S U M É

On considère une classe de problèmes paraboliques multi-échelles dont les coefficients de diffusion oscillent rapidement en espace à une échelle ε possiblement petite. Les méthodes numériques d'homogénéisation sont populaires pour ces problèmes, car elles capturent efficacement le comportement asymptotique lorsque $\varepsilon \rightarrow 0$, sans utiliser une discrétisation spatiale aussi fine que l'échelle des oscillations rapides, comme le nécessiteraient les méthodes non raides standard. Cependant, les schémas d'homogénéisation existants ne sont en général pas précis dans les deux régimes oscillant $\varepsilon \rightarrow 0$ et non oscillant $\varepsilon \sim 1$. Dans ce travail, nous introduisons une méthode *Asymptotic Preserving* basée sur une décomposition micro–macro exacte, qui reste consistante pour les deux régimes.

© 2015 Académie des sciences. Published by Elsevier Masson SAS. All rights reserved.

E-mail addresses: nicolas.crouseilles@inria.fr (N. Crouseilles), mohammed.lemou@univ-rennes1.fr (M. Lemou), Gilles.Vilmart@unige.ch (G. Vilmart).

<http://dx.doi.org/10.1016/j.crma.2015.11.010>

1631-073X/© 2015 Académie des sciences. Published by Elsevier Masson SAS. All rights reserved.

Version française abrégée

L'objectif est de construire des schémas numériques pour des problèmes paraboliques (1) où les coefficients de diffusion sont hautement oscillants en espace. Ce type de modèle intervient dans des problèmes de propagation en milieux exhibants une structure périodique. Dans de nombreux cas, la taille de la période est petite par rapport à la taille caractéristique du milieu, et en désignant par ε leur rapport, une analyse asymptotique est nécessaire pour étudier le comportement de la solution quand $\varepsilon \rightarrow 0$. Cette analyse a été conduite dans [4,5,3,10] à l'aide de la convergence double échelle.

D'un point de vue numérique, une approche directe s'avère très coûteuse, puisque les paramètres numériques des maillages doivent résoudre la plus petite échelle ε . Les méthodes numériques d'homogénéisation comme la *heterogeneous multiscale method* (HMM) [7] (voir [2] dans le contexte de problèmes paraboliques linéaires, et l'article de revue [1]) permettent de calculer efficacement la solution homogénéisée u^0 , mais aussi la solution oscillante u^ε à ε fixé en se basant sur l'approximation du modèle asymptotique, qui suppose que ε est très petit, ainsi que des techniques de correcteurs [5,10]. Cependant, si ε n'est pas petit, ce type d'approche tombe en défaut.

Dans ce travail, nous proposons une méthode qui permet d'approcher la solution u^ε pour n'importe quelle valeur de $\varepsilon \in (0, 1]$, à paramètres numériques fixés indépendamment de ε . Ce type d'approche est dit *Asymptotic Preserving* [11] : un tel schéma est cohérent avec le problème initial pour tout ε fixé et dégénère quand $\varepsilon \rightarrow 0$ en un schéma numérique cohérent avec le modèle asymptotique.

Notre approche est basée sur une reformulation du problème initial en un problème augmenté (voir (5) et les notations (6)) satisfait par $U^\varepsilon(t, x, y)$, dans lequel les échelles lentes x et rapides $y = x/\varepsilon$ sont considérées indépendantes. La solution $u^\varepsilon(t, x)$ du problème initial peut alors être retrouvée grâce à la relation $U^\varepsilon(t, x, y = x/\varepsilon) = u^\varepsilon(t, x)$. Dans le problème (5), une raideur apparaît devant le terme $LU^\varepsilon = \nabla_y \cdot (a(x, y)\nabla_y U^\varepsilon)$, qui permet de s'inspirer de méthodes de développement asymptotique largement utilisées en théorie cinétique pour construire des schémas numériques multi-échelles (voir [13]). Nous décomposons en effet la solution du problème augmenté U^ε sous la forme $U^\varepsilon(t, x, y) = F^\varepsilon(t, x) + G^\varepsilon(t, x, y)$, où F^ε est la projection orthogonale de U^ε sur le noyau de L . Cette décomposition permet de reformuler de façon équivalente le problème augmenté en un système d'équations micro-macro satisfait par F^ε et G^ε . Notons que ce système ne contient aucune approximation et reste exact pour toute valeur de ε .

Nous nous basons ensuite sur cette décomposition pour construire un schéma numérique multi-échelles. Grâce à une discrétisation en temps semi-implicite (inspirée de [13]), un schéma *Asymptotic Preserving* est alors obtenu. Ce schéma nécessite l'inversion au niveau numérique de l'opérateur L (à x fixé), comme dans le cas de la résolution numérique du problème homogénéisé (voir [7]).

Bien que la méthodologie soit présentée ici en dimension quelconque, nous effectuons des tests numériques uniquement en dimension 1. Le bon comportement du schéma pour différents $\varepsilon \in (0, 1]$ est mis en évidence en le comparant à une méthode directe et à la solution du problème homogénéisé. L'analyse du cas multi-dimensionnel avec une méthode d'éléments finis est en cours d'étude. Cette note constitue une version abrégée d'un travail plus détaillé [6].

1. Introduction

For $T > 0$ and a smooth bounded domain $\Omega \subset \mathbb{R}^d$, we consider the following class of parabolic problems

$$\partial_t u^\varepsilon = \nabla_x \cdot [a(x, x/\varepsilon)\nabla_x u^\varepsilon] + f(t, x), \quad t \in (0, T), \quad x \in \Omega, \quad (1)$$

where $u^\varepsilon(t = 0, x) = g(x)$ is a given initial condition in $L^2(\Omega)$, $f \in L^2(0, T, L^2(\Omega))$ is a given source term, and we take for simplicity homogeneous Dirichlet boundary conditions $u^\varepsilon = 0$ in $(0, T) \times \partial\Omega$. The tensor $a(x, y) \in \mathbb{R}^{d \times d}$ is assumed symmetric, uniformly elliptic and bounded, and periodic with respect to the variable $y = x/\varepsilon \in Y = (0, 1)^d$. The homogenization analysis as $\varepsilon \rightarrow 0$ of such a multiscale problem is well known and can be done using a two-scale convergence analysis, see [4,5,3,10]. The problem (1) admits a unique solution u^ε in the space $L^2(0, T; H_0^1(\Omega))$, which converges towards an asymptotic solution u^0 as $\varepsilon \rightarrow 0$,

$$u^\varepsilon \rightarrow u^0 \text{ strongly in } L^2(0, T; L^2(\Omega)), \quad u^\varepsilon \rightharpoonup u^0 \text{ weakly in } L^2(0, T; H_0^1(\Omega)),$$

where $u^0 \in L^2(0, T; H_0^1(\Omega))$ solves an effective non-oscillatory problem of the same form as (1),

$$-\nabla_y \cdot [a(x, y)[\nabla_x u^0 + \nabla_y u_1]] = 0, \quad x \in \Omega, \quad y \in Y, \quad (2)$$

$$\partial_t u^0 - \nabla_x \cdot \left[\int_Y a(x, y)[\nabla_x u^0 + \nabla_y u_1] dy \right] = f, \quad x \in \Omega, \quad (3)$$

with the same initial and boundary conditions for u^0 in (3) as for u^ε and involving the elliptic "cell problem" (2) with solution $u_1(t, x, \cdot) \in H_{\text{per}}^1(Y)$, periodic with zero average with respect to the second variable y . Taking advantage of the separation of micro- and macroscales, numerical homogenization methods exploit the above homogenization result to compute efficiently the solution to (1) in the asymptotic regime $\varepsilon \rightarrow 0$. For instance, such an efficient method is the heterogeneous

Multiscale Method (HMM) [7] (see also the review [1]), which relies on a coupling of micro and macro finite-element methods applied to (2)–(3) (see [2] in the context of parabolic multiscale problems (1)). Having a computational cost independent of the smallness of ε , HMM permits to approximate not only the asymptotic solution u^0 , but also the oscillatory solution u^ε and its gradient $\nabla_x u^\varepsilon$ for a fixed small ε using the approximation $u^\varepsilon(t, x) \simeq u^0(t, x) + \varepsilon u_1(t, x, y = x/\varepsilon)$ based on corrector techniques. The latter approximation of u^ε is consistent only for small values of ε , but not for ε close to 1. We also mention the “multiscale finite-element method” (msFEM) [9] (see the review [8]), which permits to compute the oscillatory solution u^ε by using an enriched finite-element space, but where the computational cost grows as $\varepsilon \rightarrow 0$. The aim of this paper is to introduce a micro–macro decomposition which permits to approximate u^ε accurately for both regimes $\varepsilon \rightarrow 0$ or $\varepsilon \sim 1$ at a cost independent of ε , in the spirit of Asymptotic Preserving schemes [11].

Remark 1. The asymptotic parabolic problem (3) is non-stiff and can be written in the form $\partial_t u^0 = \bar{D}u^0 + f$ where $\bar{D}\phi = \nabla_x \cdot (a^0 \nabla_x \phi)$ and a^0 is the so-called homogenized tensor. In other words, the asymptotic problem has the same form as (1) with a^ε replaced by a^0 . In dimension $d = 1$, the homogenized tensor is given by the harmonic average $a^0(x) = (\int_Y a(x, y)^{-1} dy)^{-1}$. However, in multiple dimensions, there is no such a simple formula. The calculation of the asymptotic diffusion coefficient $a^0(x)$ at a point x of space then requires the resolution of an elliptic-type problem like (2). We refer the reader to the review [1].

2. Exact micro–macro decomposition

In this section, we introduce a micro–macro decomposition of the oscillatory solution u^ε of (1), which remains exact for all $\varepsilon \in (0, 1)$, and we study its behavior for $\varepsilon \rightarrow 0$. We emphasize that our analysis is only formal, and a rigorous study of the approach is currently under investigation [6]. In the spirit of two-scale convergence analysis, we introduce a function $U^\varepsilon : (0, T) \times \Omega \times Y \rightarrow \mathbb{R}$, periodic with respect to the third variable $y \in Y = (0, 1)^d$, and such that U^ε coincides with u^ε , the solution to (1), on the diagonal, i.e.

$$U^\varepsilon(t, x, x/\varepsilon) = u^\varepsilon(t, x), \tag{4}$$

and we obtain that U^ε solves the following augmented problem

$$\partial_t U^\varepsilon = \frac{1}{\varepsilon^2} L U^\varepsilon + \frac{1}{\varepsilon} B U^\varepsilon + D U^\varepsilon + f. \tag{5}$$

Here, we use the following notations for all functions ϕ ,

$$L\phi = \nabla_y \cdot [a(x, y) \nabla_y \phi], \quad D\phi = \nabla_x \cdot [a(x, y) \nabla_x \phi], \quad B\phi = \nabla_x \cdot [a(x, y) \nabla_y \phi] + \nabla_y \cdot [a(x, y) \nabla_x \phi]. \tag{6}$$

We then choose appropriate initial and boundary conditions for (5),

$$U^\varepsilon(0, x, y) = g(x) \text{ for } x \in \Omega, y \in Y, \quad U^\varepsilon(t, x, y) = \varepsilon \left(u_1(t, x, y) - u_1(t, x, \frac{x}{\varepsilon}) \right) \text{ for } t \in (0, T), x \in \partial\Omega, y \in Y, \tag{7}$$

where u_1 is given by (2). Consider now the linear operator L in (6) defined for a fixed x on $H^1_{\text{per}}(Y)$, the space of periodic functions in $H^1(Y)$; this operator is self-adjoint with respect to the $L^2(Y)$ scalar product. Its kernel is the set of constant functions (with respect to y) and the L^2 orthogonal projector on this kernel is the average projection operator $\Pi\phi := \int_Y \phi(y) dy$. Moreover, L is an isomorphism between the Hilbert space $W_{\text{per}}(Y) = \{\phi \in H^1_{\text{per}}(Y); \Pi\phi = 0\}$ and its dual $(W_{\text{per}}(Y))'$. Following [13], in the context of kinetic theory, we now perform an exact micro–macro decomposition of U^ε by setting $F^\varepsilon = \Pi U^\varepsilon$, $G^\varepsilon = (I - \Pi)U^\varepsilon$, where I is the identity operator

$$U^\varepsilon(t, x, y) = F^\varepsilon(t, x) + G^\varepsilon(t, x, y). \tag{8}$$

Inserting this decomposition into (5), and applying respectively Π and $(I - \Pi)$, lead to the following model for the micro–macro decomposition of $u^\varepsilon(t, x) = F^\varepsilon(t, x) + G^\varepsilon(t, x, x/\varepsilon)$,

$$\begin{aligned} \partial_t F^\varepsilon &= \frac{1}{\varepsilon} \Pi B G^\varepsilon + \Pi D F^\varepsilon + \Pi D G^\varepsilon + f, \\ F^\varepsilon(0, x) &= g(x), x \in \Omega, \quad F^\varepsilon(t, x) = -\varepsilon u_1(t, x, \frac{x}{\varepsilon}), \quad t \in (0, T), x \in \partial\Omega, \end{aligned} \tag{9}$$

$$\begin{aligned} \partial_t G^\varepsilon &= \frac{1}{\varepsilon^2} L G^\varepsilon + \frac{1}{\varepsilon} (I - \Pi) B [F^\varepsilon + G^\varepsilon] + (I - \Pi) D (F^\varepsilon + G^\varepsilon), \\ G^\varepsilon(0, x, y) &= 0, x \in \Omega, y \in Y, \quad G^\varepsilon(t, x, y) = \varepsilon u_1(t, x, y), \quad t \in (0, T), x \in \partial\Omega, y \in Y, \end{aligned} \tag{10}$$

where u_1 is given in (2), and we note that $\Pi B\phi = 0$ for all ϕ independent of y .

We now study formally the asymptotic limits of G^ε and $F^\varepsilon \rightarrow \bar{F}$ as $\varepsilon \rightarrow 0$. Multiplying both sides of (10) by ε , using $\partial_t G^\varepsilon = \mathcal{O}(1)$ and setting formally $\varepsilon \rightarrow 0$, we deduce

$$\varepsilon^{-1} G^\varepsilon \rightarrow -L^{-1} B \bar{F}. \tag{11}$$

Injecting (11) into (9) we deduce formally the asymptotic limit as $\varepsilon \rightarrow 0$,

$$\partial_t \bar{F} = \bar{D} \bar{F} + f, \text{ with } \bar{D} \phi := -\Pi B L^{-1} B \phi + \Pi D \phi. \quad (12)$$

Comparing with the homogenized problem (2)–(3), we emphasize that the asymptotic limits as $\varepsilon \rightarrow 0$ in (11) and (12) coincide respectively with u^0 and u_1 in (2), (3). Precisely, we have $F^\varepsilon \rightarrow \bar{F} = u^0$ and $\varepsilon^{-1} G^\varepsilon \rightarrow -L^{-1} B u^0 = u_1$ for $\varepsilon \rightarrow 0$, and we see that the parabolic effective problem (3) is equivalent to (12). Therefore, the decomposition (4)–(8) of $u^\varepsilon(t, x)$ into the non-oscillatory part $F^\varepsilon(t, x)$ and the oscillatory part $G^\varepsilon(t, x, x/\varepsilon)$ can indeed be interpreted as a generalization for $\varepsilon \in (0, 1)$ of the approximation $u^\varepsilon \simeq u^0 + \varepsilon u_1$, valid only for small values of ε .

Remark 2. Notice that using the simpler homogeneous boundary condition $U(t, x, y) = 0$ for $t \in (0, T)$, $x \in \partial\Omega$, $y \in Y$ (instead of (7)) would yield an undesired boundary layer. Indeed, it is a classical issue for corrector techniques (see [10]) that the limit $u_1(x, y)$ appearing in (11) with $y = x/\varepsilon$ does not satisfy homogeneous Dirichlet boundary conditions for $x \in \partial\Omega$.

3. Asymptotic Preserving numerical method

The main goal of this section is to propose an Asymptotic Preserving numerical method for (9)–(10), used to approximate the solution u^ε of (1), and with a computational cost independent of $\varepsilon \in (0, 1)$. We focus on the time discretization, considering a mesh of the time interval $[0, T]$: $t^n = n\Delta t$, with $n \in \mathbb{N}$ and Δt the time step. Then, we denote by F^n (resp. G^n) an approximation of $F^\varepsilon(t^n)$ (resp. $G^\varepsilon(t^n)$).

The stiffest term in (10) has to be considered implicit to ensure stability as $\varepsilon \rightarrow 0$ whereas all the other terms can be considered explicit. Then, a natural first-order time discretization of (10) is (see [13])

$$G^{n+1} = \left(I - \frac{\Delta t}{\varepsilon^2} L \right)^{-1} \left[G^n + \frac{\Delta t}{\varepsilon} (I - \Pi)(B + \varepsilon D)(F^n + G^n) \right]. \quad (13)$$

Now, to recover the correct asymptotic behavior, the time discretization of (9) is

$$F^{n+1} = F^n + \frac{\Delta t}{\varepsilon} \Pi B G^{n+1} + \Delta t \Pi D (F^n + G^{n+1}) + f. \quad (14)$$

To make explicitly appear the asymptotic model, we now propose a suitable transformation of the macro part (14) (following [12]). To do that, we consider the following Duhamel formula for (10)

$$\partial_t (e^{-tL/\varepsilon^2} G^\varepsilon) = e^{-tL/\varepsilon^2} \left[\frac{1}{\varepsilon} (I - \Pi)(B F^\varepsilon + B G^\varepsilon) + (I - \Pi)(D F^\varepsilon + D G^\varepsilon) \right].$$

Integrating between t^n and t^{n+1} and performing some first order (in time) approximation leads to

$$\begin{aligned} G^{n+1} &\approx e^{\Delta t L/\varepsilon^2} G^n + \frac{1}{\varepsilon} \int_{t^n}^{t^{n+1}} e^{(t^{n+1}-s)L/\varepsilon^2} ds (I - \Pi) B F^n \\ &\quad + \frac{1}{\varepsilon} \int_{t^n}^{t^{n+1}} e^{(t^{n+1}-s)L/\varepsilon^2} ds (I - \Pi) B G^n + \int_{t^n}^{t^{n+1}} e^{(t^{n+1}-s)L/\varepsilon^2} ds (I - \Pi)(D F^n + D G^n). \end{aligned} \quad (15)$$

Now, our goal is to derive an approximation of G^{n+1} which will be inserted in the right-hand side of (14). This means that, in the approximation of G^{n+1} , any term of the order of Δt can be neglected if needed.

In this spirit, the time integrals in (15) are approximated as follows. The first one is calculated exactly to get $\int_{t^n}^{t^{n+1}} e^{(t^{n+1}-s)L/\varepsilon^2} ds = -\varepsilon^2 (1 - e^{\Delta t L/\varepsilon^2}) L^{-1}$, whereas the second and the third ones are approximated using a midpoint formula $\int_{t^n}^{t^{n+1}} e^{(t^{n+1}-s)L/\varepsilon^2} ds \approx \Delta t e^{\Delta t L/(2\varepsilon^2)}$. Additionally, for non-small ε , up to terms of order Δt , $e^{\Delta t L/\varepsilon^2}$ can be replaced by $e^{-\Delta t/\varepsilon^2}$; for small ε , both $e^{\Delta t L/\varepsilon^2}$ and $e^{-\Delta t/\varepsilon^2}$ go to zero. Therefore, $e^{\Delta t L/\varepsilon^2}$ may be replaced by $e^{-\Delta t/\varepsilon^2}$. Let us emphasize that all the approximations are consistent in time with the continuous model. Finally, we get

$$\begin{aligned} G^{n+1} &= e^{-\Delta t/\varepsilon^2} G^n - \varepsilon (1 - e^{-\Delta t/\varepsilon^2}) L^{-1} (I - \Pi) B F^n + \frac{\Delta t}{\varepsilon} e^{-\Delta t/(2\varepsilon^2)} (I - \Pi) B G^n \\ &\quad + \Delta t e^{-\Delta t/(2\varepsilon^2)} (I - \Pi)(D F^n + D G^n). \end{aligned}$$

This expression of G^{n+1} is injected in (14) and using $-\Pi B L^{-1} (I - \Pi) B F^n + \Pi D F^n = \bar{D} F^n$, we have

$$F^{n+1} = F^n + \Delta t (1 - e^{-\Delta t/\varepsilon^2}) \bar{D} F^n + \Delta t e^{-\Delta t/\varepsilon^2} \Pi D F^n + \frac{\Delta t e^{-\Delta t/\varepsilon^2}}{\varepsilon} \Pi B G^n + \Delta t \Pi D G^{n+1} + \Delta t f. \quad (16)$$

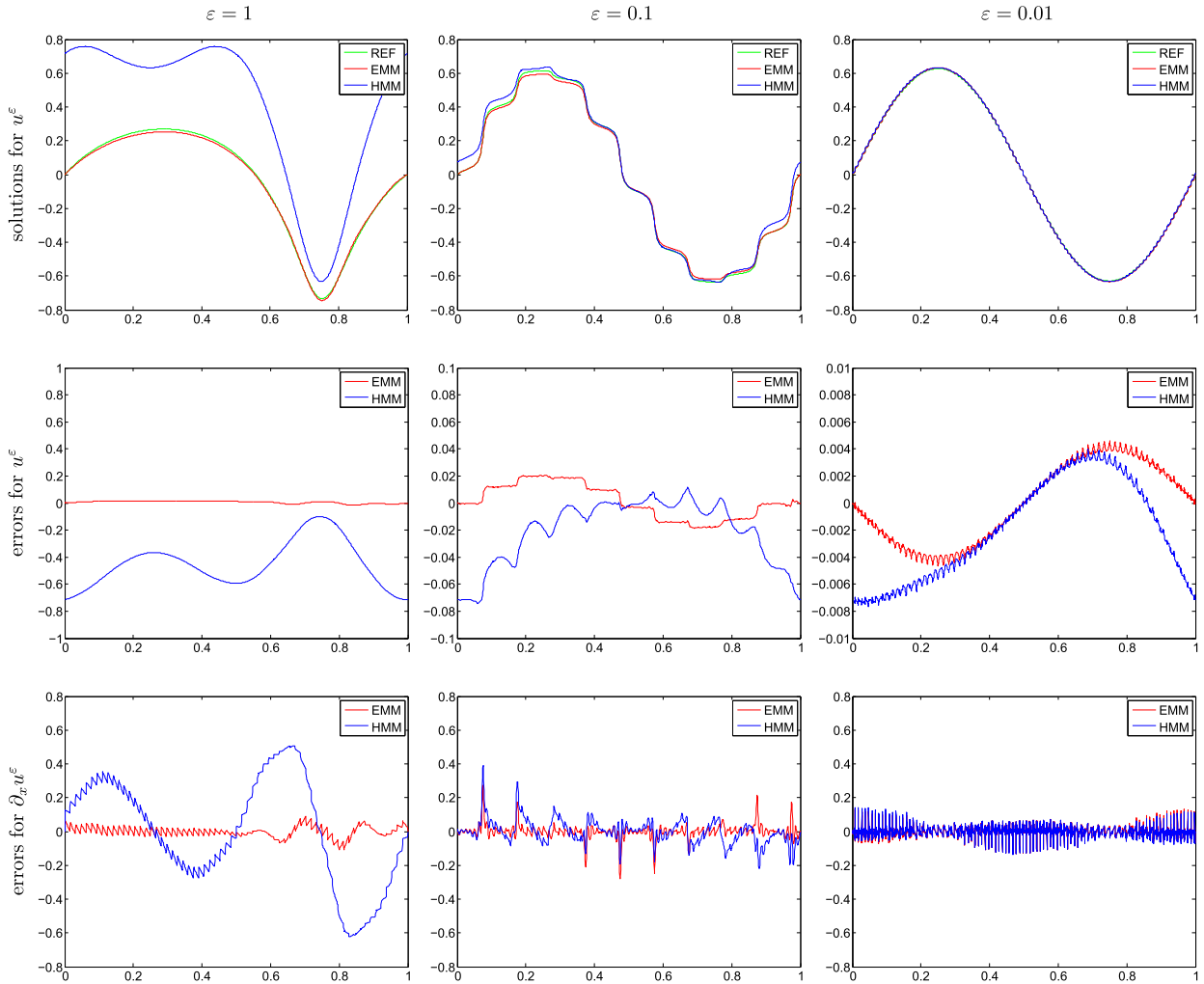


Fig. 1. First line: comparison between u_{REF} (green line), u_{EMM} (red line) and u_{HMM} (blue line) for $\varepsilon = 1, 0.1, 0.01$ (from left to right). Second line (errors in u^ε): $u_{\text{REF}} - u_{\text{EMM}}$ (red line) and $u_{\text{REF}} - u_{\text{HMM}}$ (blue line) for $\varepsilon = 1, 0.1, 0.01$ (from left to right). Third line (errors in $\partial_x u^\varepsilon$): $\partial_x u_{\text{REF}} - \partial_x u_{\text{EMM}}$ (red line) and $\partial_x u_{\text{REF}} - \partial_x u_{\text{HMM}}$ (blue line) for $\varepsilon = 1, 0.1, 0.01$ (from left to right). The EMM and HMM solutions and their derivatives are computed using the interpolation (17).

The numerical scheme (13)–(16) enjoys the Asymptotic Preserving property: (i) for a fixed $\varepsilon > 0$, it is a first-order approximation of (9)–(10); (ii) for a fixed Δt , (13)–(16) is uniformly stable with respect to ε and degenerates into a consistent discretization of the asymptotic model (12).

Note that up to first-order terms in Δt , an implicit time discretization for the term \overline{DF} could also be considered (or alternatively an explicit stabilized method as in [2]), which enables to avoid the parabolic CFL condition in the asymptotic regime. Let us also remark that the numerical scheme (13)–(16) only requires the inversion of the elliptic-type operator in dimension d , which is also needed for the numerical resolution of the asymptotic model (12). Hence, the additional computation induced by our approach only lies in the numerical approximation of Π, B, D .

4. Numerical results

We consider a simpler case to illustrate the efficiency of our approach, considering (1) in dimension $d = 1$ together with the following diffusion coefficient $A(x/\varepsilon) = 1.1 + \sin(x/\varepsilon)$ and a null right-hand side $f(x) = 0$ with the initial condition $g(x) = \sin(2\pi x)$, $x \in [0, 1]$. We then compare three different approaches for approximating the solution u^ε to (1): (i) a direct approach ('REF') based on a first-order explicit time integrator of (1), in which the mesh parameters are adapted to the smallness of ε (this will serve as a reference for comparison; obviously, another time integrator can be used, such as an implicit one); (ii) the exact micro-macro decomposition approach ('EMM') based on (13)–(16), and (iii) the asymptotic model ('HMM') $u^\varepsilon \simeq u^0 + \varepsilon u_1$ with u^0, u_1 given by (2)–(3). The spatial discretization (in x and y directions) is performed using a standard second-order finite-volume method. We denote by N_x (resp. N_y) the number of points in the x (resp. y) direction,

and $\Delta x = 1/N_x$, $\Delta y = 1/N_y$ are the mesh size in x and y directions. For REF, we choose $\Delta t = 0.05 \Delta x^2$ where Δx will be chosen small enough to capture the oscillations of size ε . For EMM and HMM, we choose $\Delta t = 0.2 \Delta x^2$. Once $U^\varepsilon(t, x, y)$ is computed on the discrete meshes, we need to interpolate it at $y = x/\varepsilon$, y being a periodic variable; this is done using trigonometric interpolation, which ensures spectral accuracy. As a diagnostic for EMM, we consider a reconstructed solution on a refined mesh by using the following linear interpolation for $x \in [x_i, x_{i+1}]$, $i = 0, \dots, N_x - 1$,

$$u^\varepsilon(t^n, x) \approx \frac{(x_{i+1} - x)}{\Delta x} \left(F^n(x_i) + G^n(x_i, \frac{x}{\varepsilon}) \right) + \frac{(x - x_i)}{\Delta x} \left(F^n(x_{i+1}) + G^n(x_{i+1}, \frac{x}{\varepsilon}) \right), \quad (17)$$

where (F^n, G^n) are given by (13)–(16), which enables us to recover the small-scale information. For HMM, we use the same reconstruction (17) with u^0 and εu_1 at $t = t_n$ (given in (2)–(3)) instead of F^n and G^n , respectively. Hence, this enables us to have an approximation of the EMM and HMM solutions as well as their spatial derivative on a refined mesh, on which the reference solution has been obtained.

In Fig. 1, we consider the cases $\varepsilon = 1, 0.1, 0.01$, respectively (from left to right). We plot at the final time $T = 1$ the solutions given by REF, EMM and HMM as functions of $x \in (0, 1)$ (first line), the error in u^ε (second line, plotting $u_{\text{REF}} - u_{\text{EMM}}$ and $u_{\text{REF}} - u_{\text{HMM}}$), and the error in the derivative $\partial_x u^\varepsilon$ (third line, plotting $\partial_x u_{\text{REF}} - \partial_x u_{\text{EMM}}$ and $\partial_x u_{\text{REF}} - \partial_x u_{\text{HMM}}$). For the reference solution REF, we use $N_x = 1024$ for $\varepsilon = 1, 0.1$, and $N_x = 4096$ for $\varepsilon = 0.01$. Concerning EMM and HMM, we use in all computations the mesh parameters $N_x = 64$ and $N_y = 16$ for all ε . We can observe that for arbitrary values of ε , EMM is in a very good agreement with the refined REF solution and its derivative, for a fixed set of numerical parameters. However, the HMM solution is accurate only in the case $\varepsilon = 0.01$. In addition, as ε goes to zero, the computational cost for EMM is constant, whereas the one of a direct method such as REF increases as the meshes need to be refined.

Acknowledgements

N.C. and M.L. acknowledge support by the ANR project Moonrise (ANR-14-CE23-0007-01). N.C. is also partly supported by the ERC Starting Grant Project GEOPARDI (ERC-279389). The research of G.V. is partially supported by the Swiss National Foundation, Grant No. 200020_144313/1.

References

- [1] A. Abdulle, W. E. B. Engquist, E. Vanden-Eijnden, The heterogeneous multiscale method, *Acta Numer.* 21 (2012) 1–87.
- [2] A. Abdulle, G. Vilmart, Coupling heterogeneous multiscale FEM with Runge–Kutta methods for parabolic homogenization problems: a fully discrete space-time analysis, *Math. Models Methods Appl. Sci.* 22 (6) (2012) 1250002.
- [3] G. Allaire, Homogenization and two-scale convergence, *SIAM J. Math. Anal.* 23 (6) (1992) 1482–1518.
- [4] A. Bensoussan, J.-L. Lions, G. Papanicolaou, *Asymptotic Analysis for Periodic Structures*, North-Holland Publishing Co., Amsterdam, 1978.
- [5] S. Brahim-Otsmane, G.A. Francfort, F. Murat, Correctors for the homogenization of the wave and heat equations, *J. Math. Pures Appl.* 71 (3) (1992) 197–231.
- [6] N. Crouseilles, M. Lemou, G. Vilmart, Asymptotic preserving numerical schemes for multiscale parabolic problems, in preparation.
- [7] W. E, B. Engquist, The heterogeneous multiscale methods, *Commun. Math. Sci.* 1 (1) (2003) 87–132.
- [8] Y. Efendiev, T.Y. Hou, *Multiscale Finite Element Methods. Theory and Applications*, Surveys and Tutorials in the Applied Mathematical Sciences, vol. 4, Springer, New York, 2009.
- [9] T.Y. Hou, X.-H. Wu, A multiscale finite element method for elliptic problems in composite materials and porous media, *J. Comput. Phys.* 134 (1) (1997) 169–189.
- [10] V. Jikov, S. Kozlov, O. Oleinik, *Homogenization of Differential Operators and Integral Functionals*, Springer-Verlag, Berlin, Heidelberg, 1994.
- [11] S. Jin, Efficient asymptotic-preserving (AP) schemes for some multiscale kinetic equations, *SIAM J. Sci. Comput.* 21 (2) (1999) 441–454 (electronic).
- [12] M. Lemou, Relaxed micro–macro schemes for kinetic equations, *C. R. Acad. Sci. Paris, Ser. I* 348 (7–8) (2010) 455–460.
- [13] M. Lemou, L. Mieussens, A new asymptotic preserving scheme based on micro–macro formulation for linear kinetic equations in the diffusion limit, *SIAM J. Sci. Comput.* 31 (1) (2008) 334–368.